Aerospace Science and Technology 157 (2025) 109854

Contents lists available at ScienceDirect

Aerospace Science and Technology

journal homepage: www.elsevier.com/locate/aescte

# Experimental study on the effects of compressor rotational speed on surge characteristics: Spatial and temporal frequencies

Ben Zhao [a], Chen Huang [a], Zhiqiang Zhang [b], Weiwei Cui [c], Teng Zhou [d,*]

[a] School of Energy Power and Mechanical Engineering, North China Electric Power University, Beijing 102206, PR China
[b] School of Mechanical Engineering, Beijing Institute of Technology, Beijing 100081, PR China
[c] Shandong University of Science and Technology, Qingdao, Shandong 266000, PR China
[d] School of Engineering, University of Southampton, Southampton SO17 1BJ, UK

ARTICLE INFO

Edited by Frank K. Lu

*Keywords:*
Compressor
Surge
Spatial frequency
Temporal frequency
Rotational speed

ABSTRACT

Surge is a significant concern in compression systems utilizing turbo-compressors as the core component, as it induces violent fluctuations in pressure and flow rate, which can potentially damage the mechanical structure. Surge characteristics can be categorized into temporal and spatial frequencies. This paper presents an experimental study of surge's temporal and spatial frequencies in both a subsonic axial compressor and a subsonic centrifugal compressor setup. A key finding of the study is the distinction between surge's spatial and temporal frequencies. The surge spatial frequency is defined as the number of surge cycles per rotor rotation (1 rad), rather than per unit time (1 s). The experimental results yield two novel conclusions: (1) surge spatial frequency is insensitive to compressor rotational speed in the experimental setups used, whereas surge temporal frequency is sensitive; (2) the surge temporal frequency exhibits a quasi-linear relationship with the compressor rotational speed across both compressor setups. The repeated observations in the two rigs suggest that this quasi-linear relationship is not an isolated occurrence. A supplementary experiment, however, disproves the universality of the quasi-linear relationship across all compressor setups. To the authors' knowledge, this is the first study to analyze surge spatial frequency, report the quasi-linear relationship, and confirm its existence in this class of compression systems.

## 1. Introduction

Compressors are employed in a wide range of engineering applications, including turbojet engines for aerospace propulsion [1], gas turbines for industrial power generation [2], automotive turbochargers [3, 4], and gas or fluid pressurization in the process industry [5]. Two boundaries limit the mass flow rate range of a compressor: one is the choking boundary, which occurs at high mass flow rates (right side) when the flow velocity near the compressor throat approaches the local speed of sound; the other is the stability boundary, which occurs at low mass flow rates (left side) and separates stable and unstable operating regimes. When the compressor operates beyond the stability boundary, it typically encounters stall or surge, leading to highly unsteady flow fluctuations, deterioration of aerodynamic performance, potential mechanical structure failure, and, in extreme cases [6], severe damage. Therefore, operational instability is a critical concern in compressor design and operation, attracting considerable research attention.

Stall and surge are distinct types of flow instability phenomena in compressors. In the case of stall, the stalled flow can propagate across a few blades and remain localized within a specific region. Previous studies have shown that the frequency of stall flow propagation is proportional to wheel speed [7]. The underlying cause of this behavior is that the propagation velocity depends on boundary-layer growth parameters. Recent research has also indicated that the frequency of blade tip leakage flow associated with stall can vary with the Reynolds number [8]. Consequently, the stall flow frequency may be influenced by operating conditions, such as the Reynolds number. In contrast, surge occurs across the entire compression system, characterized by violent airflow oscillations and pressure pulsations throughout the machine. Surge is marked by large-amplitude, low-frequency oscillations of mass flow along the streamwise direction [9], making it a higher-risk phenomenon compared to stall. However, research on surge characteristics remains limited.

Depth is a key characteristic of surge, representing its intensity.

* Corresponding author.
*E-mail address:* t.zhou@soton.ac.uk (T. Zhou).

https://doi.org/10.1016/j.ast.2024.109854
Received 29 August 2024; Received in revised form 5 December 2024; Accepted 5 December 2024
Available online 9 December 2024
1270-9638/© 2024 The Author(s). Published by Elsevier Masson SAS. This is an open access article under the CC BY license (http://creativecommons.org/licenses/by/4.0/).

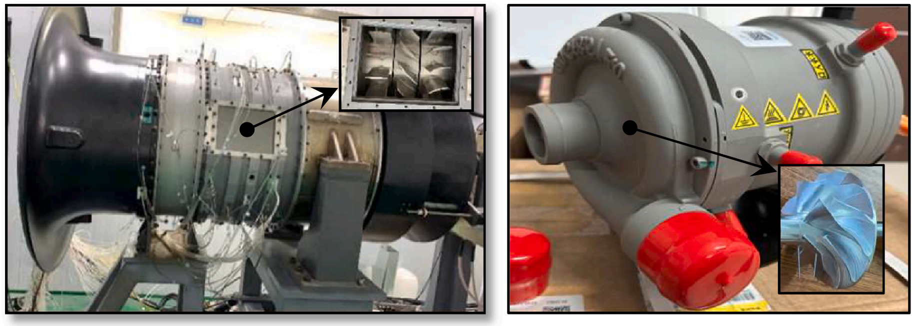

(a) Axial compressor (b) Centrifugal compressor

**Fig. 1.** Schematics of the compressors tested in this study.

Surge in practical facilities can manifest in various forms, such as mild and deep surges. Mild surge typically refers to a phenomenon where only pressure and flow fluctuations are observed within the compression system, and also called soft surge. In contrast, deep surge, as a more severe instability, is characterized by reverse flow within the system. Lou et al. [10] reported deep surge occurring at subsonic and supersonic impeller tip relative Mach numbers, while mild surge is observed when the tip relative Mach number approaches unity. They concluded that the compressor surge signature changes as the impeller inlet tip flow transitions from subsonic to supersonic conditions [10]. Further analysis revealed a spike-type deep surge at subsonic and supersonic impeller inlet tip conditions, and a modal-type mild surge at 90 % speed with transonic inlet tip conditions [11]. Due to the challenges in conducting surge experiments, Zhang et al. [12] proposed a numerical method to simulate surge oscillation characteristics. Their results indicated that the discrepancy in surge boundaries between experimental and numerical results varies at three different rotational speeds. In principle, the flow state around the impeller inlet tip is largely dependent on the compressor rotational speed, suggesting a potential relationship between surge depth and compressor speed.

Frequency is another important characteristic of surge, representing the number of surge events that occur repeatedly per unit scale. In terms of time scale, surge frequency (measured in Hz) is related to the Helmholtz frequency [13], although a significant difference often exists between the two. For example, Dehner et al. [14] reported mild surge oscillations occurring at the Helmholtz resonance frequency of the system as the compressor mass flow rate was reduced below the peak pressure ratio for a given speed. By further reducing the flow rate, they observed deep surge at a frequency well below the Helmholtz resonance. This observation suggests that surge frequency is not a constant value, even for a given system, and that factors influencing Helmholtz resonance could also affect surge frequency. Wang et al. [15] numerically assessed the surge characteristics of an axial compressor operating under surge conditions at a fixed rotational speed, finding that the oscillation frequency of the airflow varied with both system volume and average mass flow rate. Similarly, the surge period was shortened by reducing pipe length or plenum volume, as reported in reference [16]. These changes in pipe length or plenum volume alter the geometry of the Helmholtz resonant cavity. In contrast, Hayashi and Cao [17] focused on compressor rotational speed, studying surge behavior in a centrifugal compressor at various speeds. They defined surge as a non-linear characteristic, where the surge margin rapidly decreases as rotational speed increases toward its maximum. Unlike changes in system geometry, compressor rotational speed is independent of pipe length or plenum volume, and therefore does not affect the Helmholtz resonant cavity geometry. Thus, compressor rotational speed appears to be a unique factor influencing surge behavior, including both temporal and spatial frequencies.

The effects of compressor rotational speed on surge characteristics, such as temporal and spatial frequencies, are not yet fully understood. This paper investigates the surge temporal and spatial frequencies in both axial and centrifugal compressor experimental setups. Surge waveforms are observed and compared at various compressor rotational speeds. The surge frequency is then categorized into two groups: spatial and temporal frequencies, each showing distinct variations in response to changes in compressor rotational speed. The remainder of this paper is organized as follows: Section 2 presents the experimental setup, Section 3 discusses the experimental results, Section 4 addresses supplementary experimental data, and the final section provides the conclusions of this study.

**Table 1**
Main parameters of the axial compressor prototype.

| | Items | Units | Parameters |
|---|---|---|---|
| 1 | IGV number | – | 33 |
| 2 | Rotor blade number | – | 35 |
| 3 | Stator blade number | – | 37 |
| 4 | Design speed | rpm | 5000 |
| 5 | Pressure ratio at the design point | – | 1.121 |
| 6 | Efficiency at the design point | – | 0.838 |
| 7 | Mass flow rate at the design point | kg/s | 15.07 |
| 8 | Inlet/outlet diameter of the hub | mm | 465.28/490.60 |
| 9 | Inlet/outlet diameter of the shroud | mm | 606.80/606.80 |

**Table 2**
Main parameters of the centrifugal compressor prototype.

| | Items | Units | Parameters |
|---|---|---|---|
| 1 | Mass flow rate at the design point | g/s | 180 |
| 2 | Pressure ratio | – | 3.90 |
| 3 | Rotational speed at design point | rpm | 80 000 |
| 4 | Design speed | rpm | 5000 |
| 5 | Work at the design point | kW | 30 |

## 2. Experimental setup

### 2.1. Compressor prototypes

This study experimentally investigates a 1.5-stage axial compressor and a centrifugal compressor. The axial compressor consists of inlet guide vanes (IGVs), a moving blade row, and stator vanes, as shown in Fig. 1(a). The stagger angles of the IGVs are all aligned with the axial direction. Fig. 1(b) illustrates the centrifugal compressor, which includes an inlet duct, a centrifugal impeller, a vaneless diffuser, and a volute. The impeller is driven by an electric motor. Table 1 and 2 present the main parameters of the axial and centrifugal compressors, respectively.

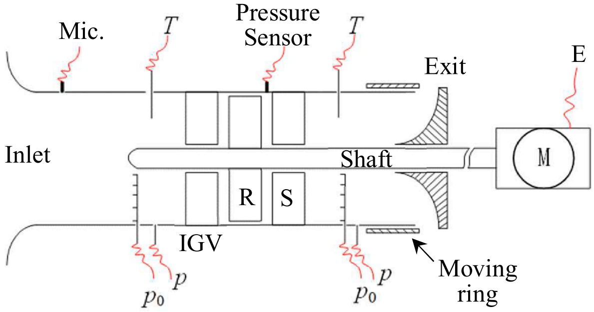


(a) The axial compressor.

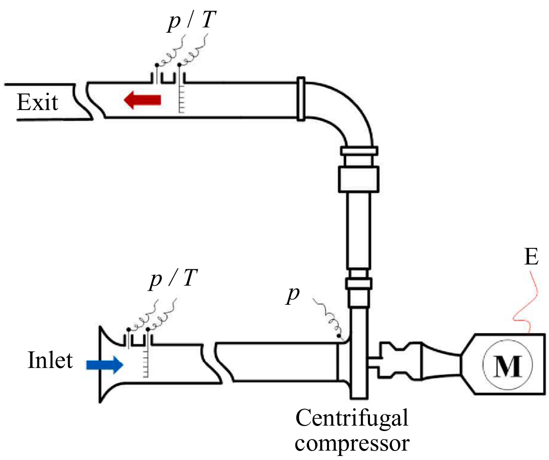


(b) The centrifugal compressor.

**Fig. 2.** Test rigs employed in the present study.

### 2.2. Test rigs

Fig. 2 illustrates the structures of the compressor test rigs used in this study. The axial compressor setup, constructed by Shandong University of Science and Technology, featured a duct with a bell-mouth nozzle at the upstream end. During the experiments, no screens or flow straighteners were used on the inlet side. In the middle section, three blade/vane rows were arranged in the IGV/R/S configuration. A shaft connected the rotor to the electric motor. Downstream of the stator, an outlet duct was used as the plenum. A movable ring was designed at the exit, and by adjusting the axial position of the ring, the flow area at the exit and thus the flow rate could be actively controlled.

The centrifugal compressor test rig, constructed at the Beijing Institute of Technology, was used in this study. As shown in Fig. 2(b), the compressor is driven by an electric motor. Total pressure, static pressure, and temperature were measured at both the inlet and outlet pipelines. Additionally, a dynamic pressure sensor was installed at the compressor inlet to monitor pressure fluctuations.

### 2.3. Measuring apparatus

In both test rigs, dynamic pressure signals, $p$, were measured using dynamic pressure transducers (Kulite brand XTL-140 M). As shown in Fig. 2, the transducers were mounted on the shroud casing of the centrifugal compressor, while in the axial compressor, they were positioned upstream of the vane, between the rotor and stator, and downstream of the stator. For each measurement, the dynamic pressure transducers were sampled at a rate of 200 kHz. The sampling duration varied depending on the test case but was always sufficient to capture the process from surge onset to retreat, including more than 30 surge cycles. Surge onset and retreat were controlled by adjusting the throttle valve.

In addition, static pressure and temperature at both the inlet and outlet of the compressors were monitored during the measurements. Static pressure was measured using strain gauge and piezoresistive transducers, which had an accuracy of 1 % of the full measurement scale. The mass flow rate was measured with a double-foil flow meter mounted at the upstream end of the compressor inlets, with a measurement accuracy of 1.5 %.

## 3. Experimental results and analysis

### 3.1. Surge operation

Fig. 3 presents the performance maps for the two compressors. The rotational speed of the axial compressor ranges from 2000 to 4500 rpm, corresponding to 40 % to 95 % of the design speed. Surge cycles were measured at 40 %, 50 %, 60 %, 70 %, 80 %, and 90 % of the design speed, as indicated in Fig. 3(a). Similarly, the centrifugal compressor was tested within a rotational speed range of 35,000 rpm to 60,000 rpm, which is within the performance map in Fig. 3(b).

In each measurement, the compressor initially operated at a near-surge point, where aerodynamic performance was degraded but surge had not yet occurred. The valve was then gradually closed to reduce the

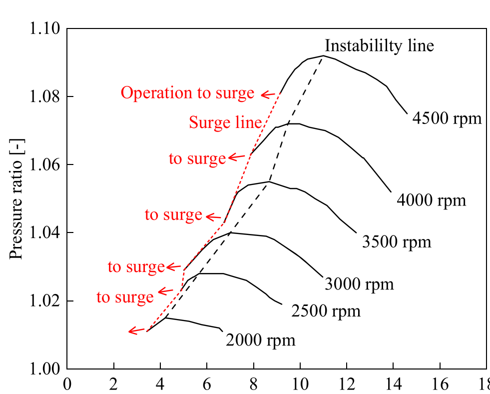


(a) Axial compressor.

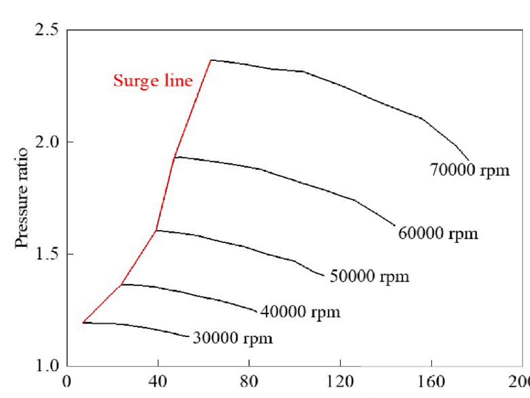


(b) Centrifugal compressor.

**Fig. 3.** Performance maps of two compressors.

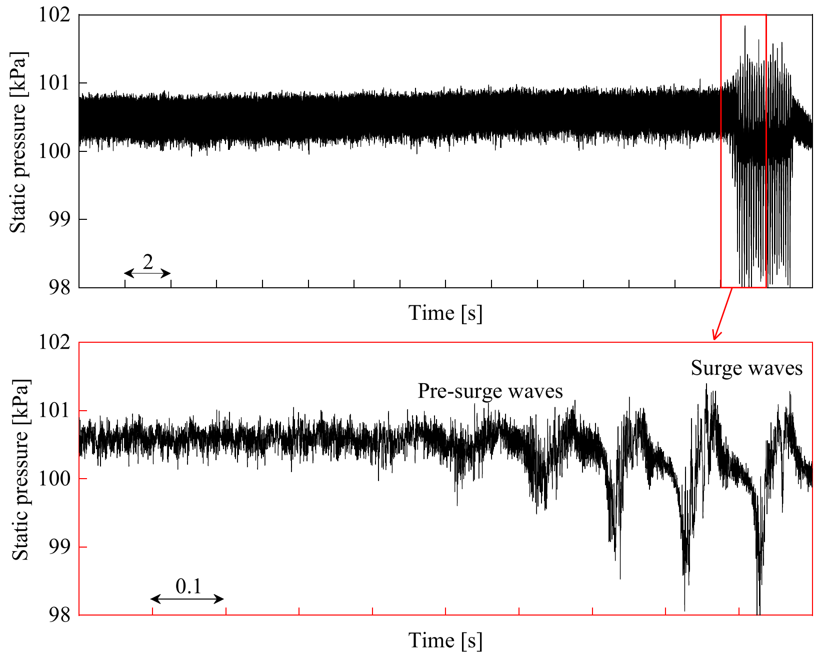


**Fig. 4.** Time sequence of the dynamic pressure measured at the axial compressor shroud casing at 2500 rpm.

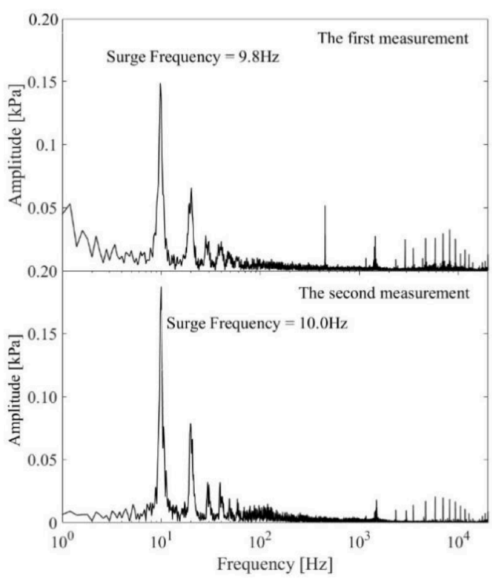


**Fig. 5.** Spectra of the dynamic pressure at the rotational speed of 2500rpm.

compressor flow rate, while the rotational speed remained constant. Once the compressor entered the surge regime, the valve opening was held steady for a brief period to allow the measurement apparatus to record the surge cycles. After at least 30 surge cycles, the valve was quickly reopened, and the compressor returned to its steady state.

Fig. 4 presents the static pressure measured from the axial compressor shroud casing at a rotational speed of 2500 rpm. The x-axis represents the time sequence, covering the process from the onset to the end of a surge. The amplitude of the pressure fluctuations increases dramatically once the surge is triggered. Prior to surge onset, as the compressor approaches the surge limit, a few pre-surge waves can be observed, as indicated by the scaled plot.

The surge wave corresponds to system vibration at a low frequency, distinct from the stall flow, which occurs in a localized region and is characterized by a relatively high frequency. Fig. 5 shows the fast Fourier transform (FFT) results of the surge signal, comparing the results of two experiments conducted on different days using the same method, at a rotational speed of 2500 rpm. The temporal frequency of the surge in the centrifugal compressor setup is nearly identical: 9.8 Hz in the first measurement and 10.0 Hz in the second measurement. The surge frequency is approximately 0.39 % of the rotor rotational temporal frequency, which is much lower than the stall temporal frequency in the axial compressor, confirming it as a surge characteristic. The deviation between two measurements is approximately 2 %, attributed to numerical errors and variations in ambient conditions. Of these two factors, the latter is likely the dominant one, as the Helmholtz resonance frequency is dependent on ambient conditions. The observed deviation is reasonable, thus demonstrating the repeatability of the experiments.

### 3.2. Surge wave

The compressor rotational speed influences the amplitude of the surge wave. Fig. 6 shows the pressure waves during surge cycles, which were filtered using a low-pass filter with a cutoff frequency set at 1.2 times the rotor rotational frequency. In other words, the filter allows signals with frequencies below the cutoff to pass through. The x-axis represents the rotor's rotating radian, with units in radians. Each subplot corresponds to a fixed compressor rotational speed, plotting the filtered signal against the rotor revolution. A comparison of the subplots reveals a gradual increase in the amplitude of the surge wave with increasing compressor rotational speed, indicating higher surge wave energy and greater risk at higher rotational speeds.

The compressor rotational speed has little effect on the surge wave patterns, except for the amplitude. The waveform consistently features a dominant peak, followed by two perturbations and a deep trough within one surge period. This pattern remains unchanged with variations in compressor rotational speed. Geometrically, the volume of the downstream plenum and the length of the prototype are constant for each measurement. Regarding the operating environment, the compressor inlet condition is assumed to be the ambient atmosphere, which remains unchanged, thus ensuring the same sound speed, isentropic exponent, and specific heat. The only variable that changes across measurements is

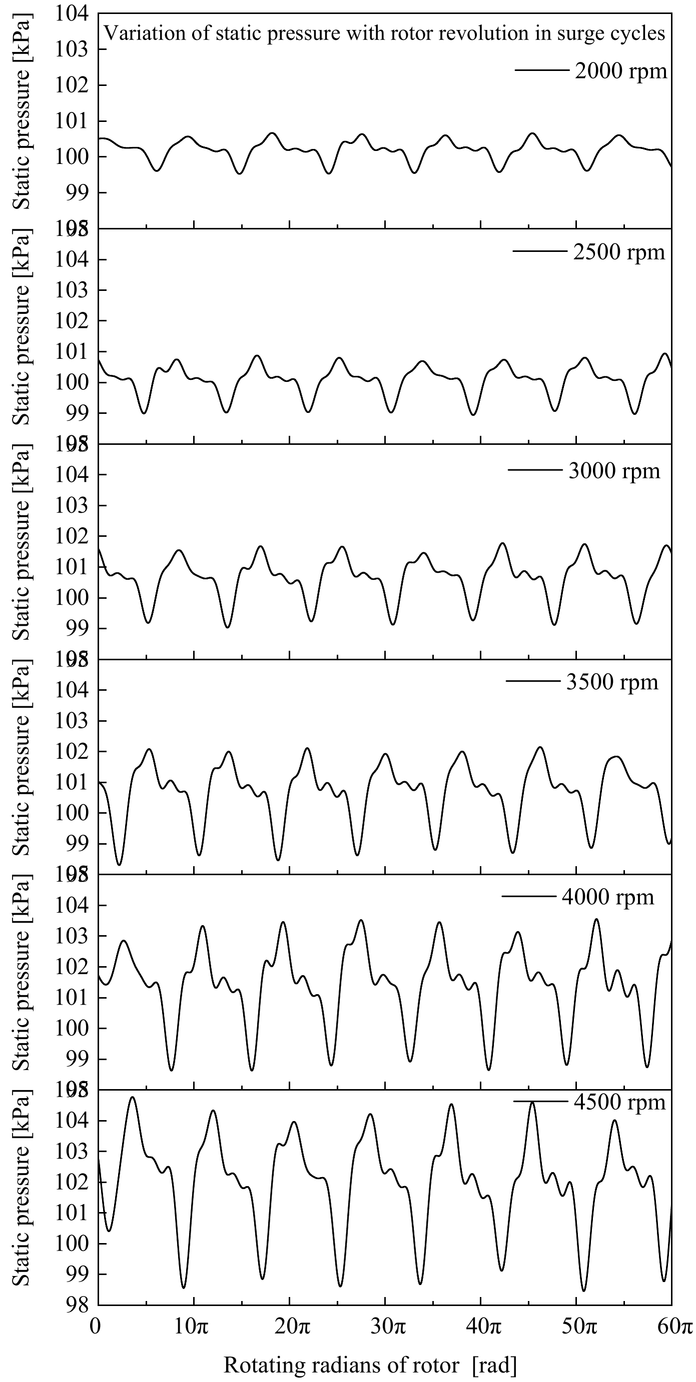


**Fig. 6.** Time sequence of the dynamic pressure signal in surge cycles (the signals are obtained using the low pass filtering method with a top limit of 1.2 times rotor rotation frequency).

the compressor rotational speed. Therefore, it can be concluded that varying the compressor rotational speed does not affect the appearance or disappearance of the perturbations in the surge waves. In other words, the surge wave perturbations are independent of the compressor rotational speed.

The compressor rotational speed has minimal effect on the spatial frequency of the surge. Fig. 7 compares the spatial frequency of surge cycles at various compressor rotational speeds. The spatial frequency represents the number of surge waveforms repeating over an angle of 1 radian, with 2π radians corresponding to one rotor revolution. The comparison of spatial frequencies shows slight variations within a deviation band of 8.86 %, indicating a low sensitivity of the surge spatial frequency to the compressor rotational speed. To the authors' knowledge, this is the first study to define surge spatial frequency and demonstrate its low sensitivity to compressor rotational speed.

### 3.3. Surge frequency

The surge temporal frequency is strongly correlated with the rotational speed. Temporal frequency refers to the number of surge waveforms that repeat per unit time (1 second). Fig. 8 depicts the dependence of surge temporal frequency on the compressor rotational frequency.

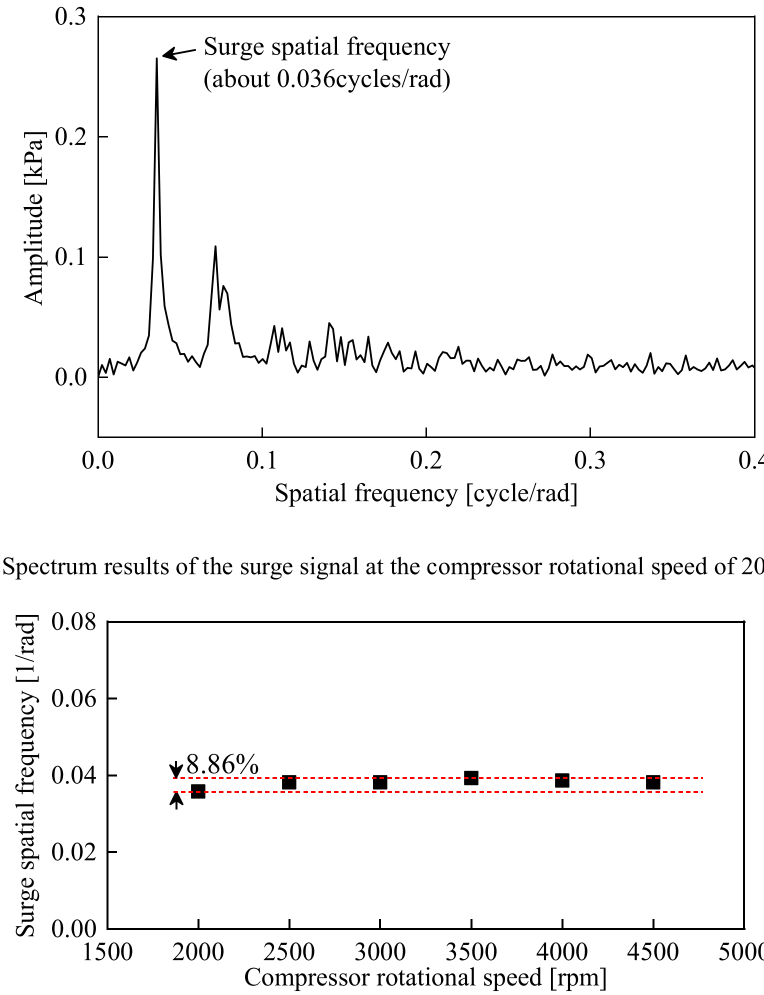


(a) Spectrum results of the surge signal at the compressor rotational speed of 2000 rpm.

(b) Spectrum results of the surge signal at various compressor rotational speeds.

**Fig. 7.** Spatial frequency of axial compressor setup surge at the rotational speed of 2000 rpm.

The compressor rotational frequency, the inverse of the compressor rotational speed, is measured in Hz, which corresponds to the units on the y-axis. The experimental results show a significant change in surge temporal frequency with the compressor rotational frequency, indicating a high sensitivity of the surge temporal frequency to the compressor rotational speed. Righi et al. [18] reported that the surge period is influenced by the reflection of the initial surge wave in the inlet duct. From this perspective, the compressor rotational speed may alter the reflection time of the initial surge wave.

The surge temporal frequency is approximately proportional to the compressor rotational frequency for the axial compressor prototype. The experimental data in Fig. 8(a) show a quasi-linear relationship between surge temporal frequencies and compressor rotational frequency. Linear fitting of the experimental data reveals a fitted line with a slope of approximately 0.25, with only slight deviations from the experimental points. To the authors' knowledge, this quasi-linear relationship is a novel finding and has not been reported in the open literature.

The quasi-linear relationship is consistently observed in the centrifugal compressor setup. Fig. 8(b) presents an additional set of experimental data as supplementary evidence. This experiment was conducted using the centrifugal compressor setup described earlier. The data from the centrifugal compressor also shows a quasi-linear relationship between surge temporal frequency and compressor rotational frequency, similar to the findings from the axial compressor setup, though with a different slope. The variation in slope can be attributed to the geometric parameters of the setup. The repeatability of these experimental results confirms that it is not uncommon for the surge temporal frequency to change with the compressor rotational frequency in a quasi-linear manner.

In summary, the analysis reveals two novel findings: (1) the surge temporal frequency is highly sensitive to the compressor rotational speed, whereas the surge spatial frequency is not; (2) the surge temporal frequency changes with the compressor rotational frequency in a quasi-linear manner. These findings are not uncommon, as they have been consistently observed in both compressor experimental setups.

## 4. Discussion

Although the quasi-linear relationship is not rare, it does not occur consistently across all experimental setups. In our previous experiment on a transonic centrifugal compressor, this quasi-linear distribution was not observed. Further details about the transonic compressor can be found in references [19–21]. In that experiment, a radial turbine was used as the power source to drive the centrifugal compressor, and it offered lower precision in controlling the compressor rotational speed compared to the electric motor used in the other setups. Table 3 presents the surge temporal frequencies at three compressor rotational speeds, revealing a non-linear relationship between surge temporal frequency and compressor rotational frequency. The precision of compressor rotational speed control is likely a contributing factor to this non-linear

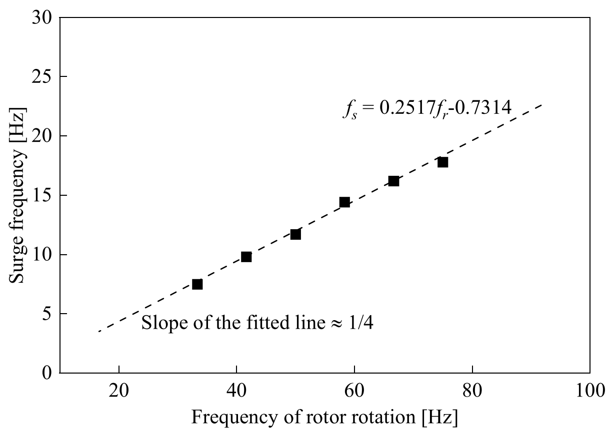


(a) axial compressor experimental setup.

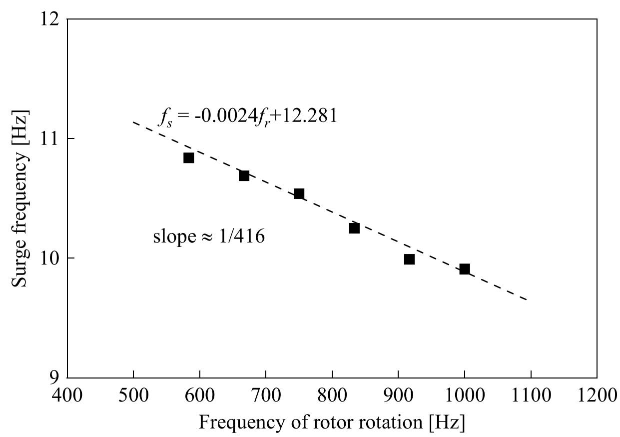


(b) Centrifugal compressor experimental setup.

**Fig. 8.** Relationship between the surge temporal frequency and rotor rotation frequency in the centrifugal compressor setup.

**Table 3**
Surge frequency of centrifugal compressor flow bench (not linearity).

| No. | Impeller rotation frequency [Hz] | Surge frequency [Hz] |
|---|---|---|
| 1 | 500.00 | 5.50 |
| 2 | 666.67 | 8.17 |
| 3 | 833.33 | 7.00 |

behavior, as compressor surge temporal frequency is closely related to rotational speed. Therefore, this case demonstrates that the quasi-linear relationship does not apply universally across all experimental setups.

The conditions that lead to the quasi-linear relationship remain unclear. There are two key differences between the compressor setups: the inlet conditions (subsonic versus transonic) and the power sources (electric motor versus turbine). In this study, when an electric motor was used, the quasi-linear relationship was observed in both the axial and centrifugal compressor setups. However, when a radial turbine was used as the power source to drive the centrifugal compressor, the relationship was not linear. At present, it is not fully understood which of these factors—either the inlet condition or the power source—contributes to the change in surge temporal frequency, or under what conditions the quasi-linear relationship occurs.

## 5. Conclusions

This paper experimentally examines the surge spatial frequency and the surge temporal frequency based on two compressor setups, an axial and a centrifugal compressor rig. The spatial frequency is characterized by the number of surge cycles per 1 rad, the rotor rotation angle. The temporal frequency stands for the surge cycle account per unit time. Their units are 1/rad and hertz (Hz), respectively.

The experimental results reveal two novel findings. First, there is a low correlation between the surge spatial frequency and the compressor rotational frequency, while the surge temporal frequency exhibits a high sensitivity to the compressor rotational frequency/speed. Second, a quasi-linear relationship is observed, where the surge temporal frequency changes with the compressor rotational frequency.

The quasi-linear relationship is not rare, but it does not apply to all compressor experimental setups, suggesting that it is limited to a specific class of setups. The repeated observation of the quasi-linear distribution in two experimental setups supports the idea that this relationship is not uncommon. However, supplementary data from an experiment conducted on a transonic centrifugal compressor using a turbocharger flow bench (in which a turbine is used as power source rather than electric motor) provides crucial evidence that the quasi-linear relationship between surge temporal frequency and compressor rotational frequency does not hold in all compressor setups.

## CRediT authorship contribution statement

**Ben Zhao:** Writing – review & editing, Writing – original draft, Supervision, Resources, Project administration, Methodology, Funding acquisition, Formal analysis, Conceptualization. **Chen Huang:** Writing – review & editing, Software, Methodology, Data curation. **Zhiqiang Zhang:** Writing – review & editing, Investigation, Data curation. **Weiwei Cui:** Writing – review & editing, Supervision, Conceptualization. **Teng Zhou:** Writing – review & editing, Validation, Methodology, Investigation, Formal analysis, Data curation.

## Declaration of competing interest

The authors declare that they have no known competing financial interests or personal relationships that could have appeared to influence the work reported in this paper.


## Acknowledgment

The authors thank the financial support supported by the Beijing Natural Science Foundation (Grant No. JQ24016) and the National Natural Science Fundamental of China (Grant No. 52006217 and 52076124).


## Data availability

Data will be made available on request.

## References


[1] T. Zou, C. Lee, The effect of the wake on the separated boundary layer in a two-stage compressor, Phys. Fluids 33 (2021) 034125.
[2] H. Tang, T. Deveney, T. Shardlow, et al., Use of Bayesian statistics to calculate transient heat fluxes on compressor disks, Phys. Fluids 34 (2022) 056108.
[3] B. Zhao, H. Sun, L. Wang, et al., Impact of inlet distortion on turbocharger compressor stage performance, Appl. Therm. Eng. 124 (2017) 393–402.
[4] B. Zhao, L. Hu, Q. Zhao, et al., Investigation of variable orifice plate design for centrifugal compressor low-end performance improvement, Aerosp. Sci. Technol. 97 (2020) 105585.
[5] H. Zeng, W. Kong, X. Zheng, A new appraisal of critical B parameter in compressor aerodynamic instability design, Aerosp. Sci. Technol. 128 (2022) 107780.
[6] J.T. Gravdahl, Modeling and control of surge and rotating stall in compressors, Department of Engineering Cybernetics, Norwegian University of Science and Technology, Norway, 1998. N-7034 TrondheimThesis, Report 98-6-W.

[7] H.W. Emmons, C.E. Pearson, H.P. Grant, Compressor surge and stall propagation, Trans. ASME. 77 (4) (1955) 455–467. May.
[8] Z. Li, J. Zhou, X. Zhu, et al., Investigation of Reynolds number effects on flow stability of a transonic compressor using a dynamic mode decomposition method, Aerosp. Sci. Technol. 153 (2024) 109421.
[9] J. Li, B. Wang, H. Yang, et al., Investigation on probe streamwise distribution for surge measurement in compression system, Aerosp. Sci. Technol. 131 (2022) 1088009.
[10] F. Lou, H.M. Harrison, N.L. Key, Investigation of surge in a transonic centrifugal compressor with vaned diffuser—part i: surge signature, ASME. J. Turbomach. 145 (5) (2023) 051003.
[11] F. Lou, H.M. Harrison, W.J. Brown, N.L. Key, Investigation of surge in a transonic centrifugal compressor with vaned diffuser: part II—correlation with subcomponent characteristics, ASME. J. Turbomach. 145 (5) (2023) 051004.
[12] M. Zhang, W. Wu, C. Zhou, Numerical model of predicting surge boundaries in high-speed centrifugal compressors, Aerosp. Sci. Technol. 141 (2023) 108518.
[13] X. Zheng, A Liu, Phenomenon and mechanism of two-regime-surge in a centrifugal compressor, ASME. J. Turbomach. 137 (8) (2015) 081007.
[14] R. Dehner, A. Selamet, P. Keller, M Becker, Simulation of deep surge in a turbocharger compression system, ASME. J. Turbomach. 138 (11) (2016) 111002.
[15] M. Wang, H. Sun, Z. Wang, Numerical investigation of the effects of system volume and average mass flow on the surge characteristics of an axial compressor, Aerosp. Sci. Technol. 106 (2020) 106172.
[16] Huang, Q., Zhang, M., Zheng, X., Compressor surge based on a 1D-3D coupled method – Part 2: surge investigation. 2019, 90: 289–298.
[17] Y. Hayashi, T Cao, An investigation of non-linear surge characteristic in a high-speed centrifugal compressor, ASME. J. Turbomach. 145 (5) (2023) 051010.
[18] M. Righi, V. Rachidis, L. Könözsy, et al., Experimental validation of a three-dimensional through-flow model for high-speed compressor surge, Aerosp. Sci. Technol. 128 (2022) 107775.
[19] B. Zhao, T. Zhou, C. Yang, Experimental investigations of centrifugal compressor surge noise, ASME J. Turbomach. 145 (8) (2023) 0810014.
[20] B. Zhao, T. Zhou, C. Yang, Experimental investigations on effects of the self-circulation casing treatment on acoustic and surge characteristics in a centrifugal compressor, Aerosp. Sci. Technol. 1331 (2022) 108002.
[21] B. Zhao, T. Zhou, L. Zhang, Investigation of dual-ported shroud casing in a centrifugal compressor: aerodynamic performance and aeroacoustics, in: Proceedings of the institution of mechanical engineers, Part C: Journal of mechanical engineering science 238, 2024, pp. 9008–9018.